The Astrophysical Journal Letters, 733:L23 (6pp), 2011 June 1 doi:10.1088/2041-8205/733/2/L23

THE FIRST OBSERVATION OF A RAPIDLY ROTATING CORONAL MASS EJECTION IN THE MIDDLE CORONA

A. Vourlidas[1], R. Colaninno[1], T. Nieves-Chinchilla[2], and G. Stenborg[3]
[1] Solar Physics Branch, Space Sciences Division, Naval Research Laboratory, Washington, DC, USA
[2] Department of Physics, Catholic University of America, Washington, DC, USA
[3] Interferometrics, Inc., Herdon, VA, USA
Received 2011 February 27; accepted 2011 April 12; published 2011 May 6

ABSTRACT

In this Letter, we present the first direct detection of a rotating coronal mass ejection (CME) in the middle corona (5–15 $R_\odot$). The CME rotation rate is 60° day^{-1}, which is the highest rate reported yet. The Earth-directed event was observed by the *STEREO*/SECCHI and *SOHO*/LASCO instruments. We are able to derive the three-dimensional morphology and orientation of the CME flux rope by applying a forward-fitting model to simultaneous observations from three vantage points (SECCHI-A, -B, LASCO). Surprisingly, we find that even such rapidly rotating CME does not result in significant projection effects (variable angular width) in any single coronagraph view. This finding may explain the prevalent view of constant angular width for CMEs above 5 $R_\odot$ and the lack of detections of rotating CMEs in the past. Finally, the CME is a "stealth" CME with very weak low corona signatures as viewed from Earth. It originated from a quiet-Sun neutral line. We tentatively attribute the fast rotation to a possible disconnection of one of the CME footpoints early in the eruption. We discuss the implications of such rotations to space weather prediction.

Key words: Sun: activity – Sun: coronal mass ejections (CMEs)

Online-only material: animation

1. INTRODUCTION

The angular width and speed are the most common properties measured to quantify coronal mass ejections (CMEs). Both parameters refer to quantities projected on the sky plane. The speed is derived through fitting of a series of height–time data points while the angular width is measured at a single height. This difference in data collection is based on the widely held assumption that the angular width of CMEs remains constant after they reach a certain height, usually above 5 $R_\odot$ (Webb et al. 1997; St. Cyr et al. 2000; Stockton-Chalk 2002). This characteristic is also referred to as radial or linear expansion in the literature. A constant angular width has been measured directly in many events (Funsten et al. 1999; Stockton-Chalk 2002). It is also supported by the similarity of *Helios* width estimates to the *Solwind* measurements (Webb & Jackson 1990) and the relative success of cone models in fitting halo CMEs (e.g., Zhao et al. 2002; Xie et al. 2004; Xue et al. 2005) under the assumption of constant cone angle or equivalently, constant CME angular width.

At the same time, there is mounting evidence for CME rotation in the low corona. It is based on observations of erupting filaments (e.g., Torok et al. 2010), theoretical considerations (Lynch et al. 2009, and references therein), and comparisons between the orientation of erupting neutral lines at the Sun and the in situ detections of magnetic clouds (Yurchyshyn et al. 2007; Yurchyshyn 2008). During the LASCO era, the rotation of CMEs in the middle and outer corona was deduced indirectly by fitting halo CMEs with elliptical cones models as a function of time. Such measurements, however, are problematic since the halo morphology arises from the CME-driven shock rather than the erupting flux rope itself (Vourlidas & Ontiveros 2009) and the derived rotation, if real, may be biased by the shock evolution. However, the observational evidence for rotation cannot be easily discounted. It is expected in almost all theoretical initiation models since many of them involve shear or helical instabilities to start the eruption. Taken together, these arguments suggest that CME rotation should be a common occurrence. Rotation should be relatively straightforward to detect in the coronagraph images as deviation from radial expansion. But this is at odds with the strong observational prevalence of CMEs with constant angular width of CMEs. Why we do not detect such nonlinear expansion in CMEs more often? Why are all such reports of CME rotation based on indirect measurements even after the observation of more than 15,000 CMEs from LASCO?

Projection effects may play a role. Indeed, since the launch of the *STEREO* mission, the number of reports of nonlinear expansion in CMEs has been increasing. Byrne et al. (2009) presented indirect evidence for nonlinear CME expansion based on measurements via an automated fitting algorithm. Lynch et al. (2010) tracked the three-dimensional (3D) morphology of a slow CME using the Thernisien et al. (2009) fitting method and measured both a nonlinear expansion and a rotation as expected. However, their measurements are not without problems. Most of the COR2 rotation measurements lie on a straight line, and the rotation becomes apparent only in the HI-1 field of view where both resolution and projection effects impede the separation between the CME flux-rope and deflected structures (Figure 8 in Lynch et al. 2010). The low rotation rate (∼19° day^{-1}) is certainly a reason for this ambiguity. More recently, Poomvises et al. (2010) reported a small nonlinear expansion of two CMEs in the order of only 10° from 5 to 40 $R_\odot$. It is, however, difficult to evaluate the significance of this measurement. It does not correlate to the actual coronagraph measurements of the projected angular width and it refers to a change in the fit parameters which is within the margin of error of the Thernisien et al. (2009) procedure used by the authors. In other words, there has not been a report of a CME that is unambiguously rotating or equivalently, expanding nonlinearly

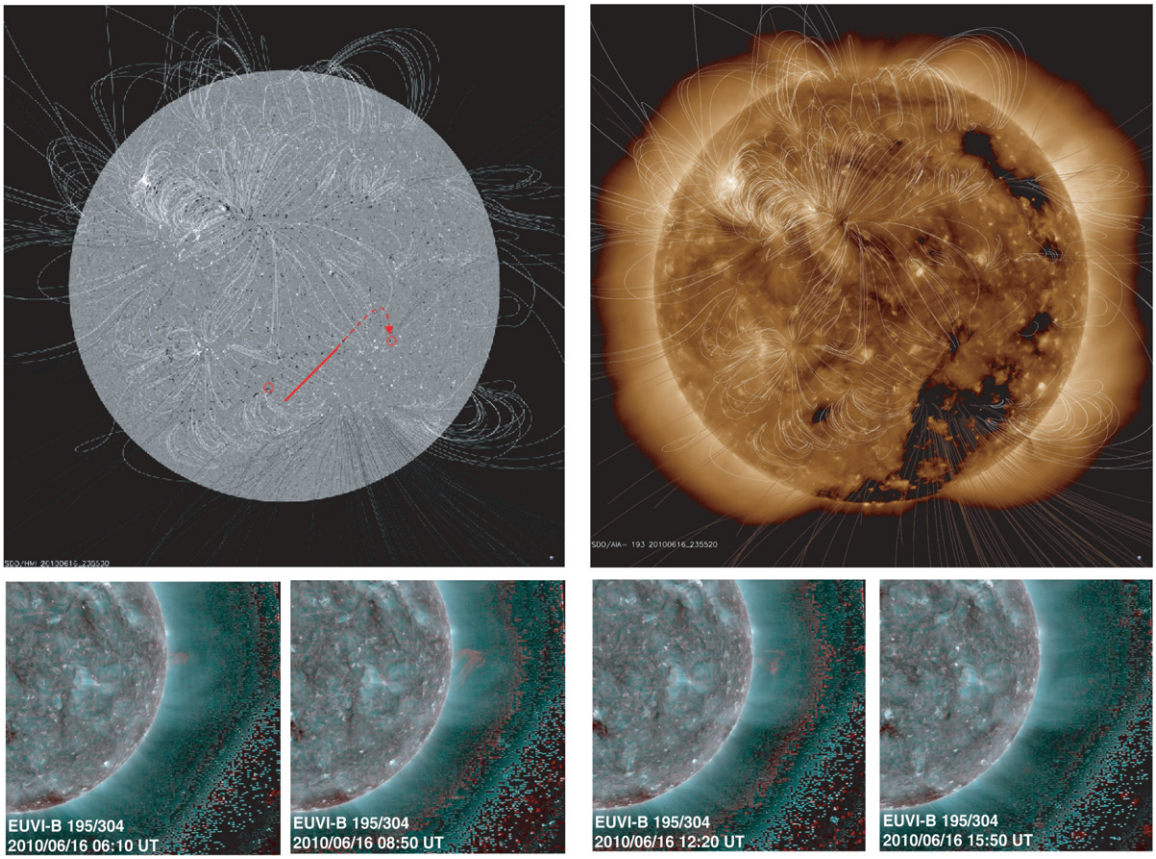

Figure 1. Solar observations of the event and its source region on 2010 June 16. Top left: HMI observation at 23:55:30 UT with superimposed field lines from a PFSS extrapolation. The source region is marked by the red line. The length of the red line approximates the length of the faint post-CME loops. The dotted red arrow marks the extent and direction of the 304 Å flows. The red circles mark the approximate locations of the flux-rope footpoints. Top right: AIA 193 Å image, at 23:55:30 UT, with the same field lines superimposed. Both *SDO* images were downloaded from the "Sun Today" Web site (sdowww.lmsal.com/suntoday). Bottom panels: selected SECCHI/EUVI-B observations of the eruption in two wavelengths, 304 Å (red) and 195 Å (silver). The images have been enhanced with the Stenborg et al. (2008) wavelet algorithm. From left to right, the images correspond to the phases of pre-event, main disconnection, post-CME heating and strong flows, and the end of the event. EUVI-B is situated 70° west from the Sun–Earth.

in the coronagraph field of view, between 5 and 30 $R_\odot$ despite the fact that such rotation is expected on both theoretical grounds and low corona observations.

We remedy the deficiency with this Letter. We report the first direct observations and measurements of a nonlinearly expanding CME and unambiguously link the observed nonlinear expansion to the rotation of the CME flux rope. The observations are described in detail Section 2 and the results are discussed in Section 3. We conclude in Section 4. Only the middle corona observations are discussed here. In a companion paper (Nieves-Chinchilla et al. 2011), we will compare the heliospheric imaging observations of this event to its in situ signatures.

CME rotation is a very important issue both for understanding the forces that drive an eruption but also for predicting the orientation of the magnetic field inside the CME. The latter has important implications for space weather predictions which so far are unable to estimate the magnetic field orientation from remote imaging of the solar source. We need to understand where or which CMEs rotate strongly and why if we ever hope to understand the geoeffectiveness of these events.

2. OBSERVATIONS AND DATA ANALYSIS

The event was observed with all telescopes of the SECCHI suite (Howard et al. 2008) on both *STEREO* spacecraft (Kaiser et al. 2008). It was Earth-directed and appeared in the COR2 field of view on 2010 June 16. On that day, the *STEREO-A* and *B* spacecraft were 74° and 70° from Earth, respectively. The event was another example of a stealth CME (Robbrecht et al. 2009) with extremely weak low corona signatures as viewed from Earth. The low corona counterpart of the eruption was, however, visible by the SECCHI/Extreme UltraViolet Imager (EUVI) telescopes which observed part of a high-lying filament (at ∼1.12 $R_\odot$ above the Earth-facing solar limb) taking off at around 06:50 UT (Figure 1, bottom left). The remaining filament rose further to about 1.2 $R_\odot$ while exhibiting strong downward flows. Eventually, that structure also erupted marking the end of the event (Figure 1, bottom right). These observations were made in 304 Å and 195 Å. The EUVI 195 Å images showed a very faint cavity overlying the erupting filament. We could see a continuous outflow during the two erupting phases of the filament and a clear off-limb depletion after the last piece was ejected. In other words, the CME did not take off instantaneously but formed over the course of about 8 hr, giving the impression that one footpoint left first and the second followed later. This observation and the downward 304 Å flows may be related to the strong rotation of this event as we discuss later.

With the aid of the EUVI observations, we were able to trace the source region in the *Solar Dynamics Observatory*/Atmospheric Imaging Assembly (*SDO*/AIA) and Helioseismic and Magnetic Imager (HMI) images (Figure 1, top panels).

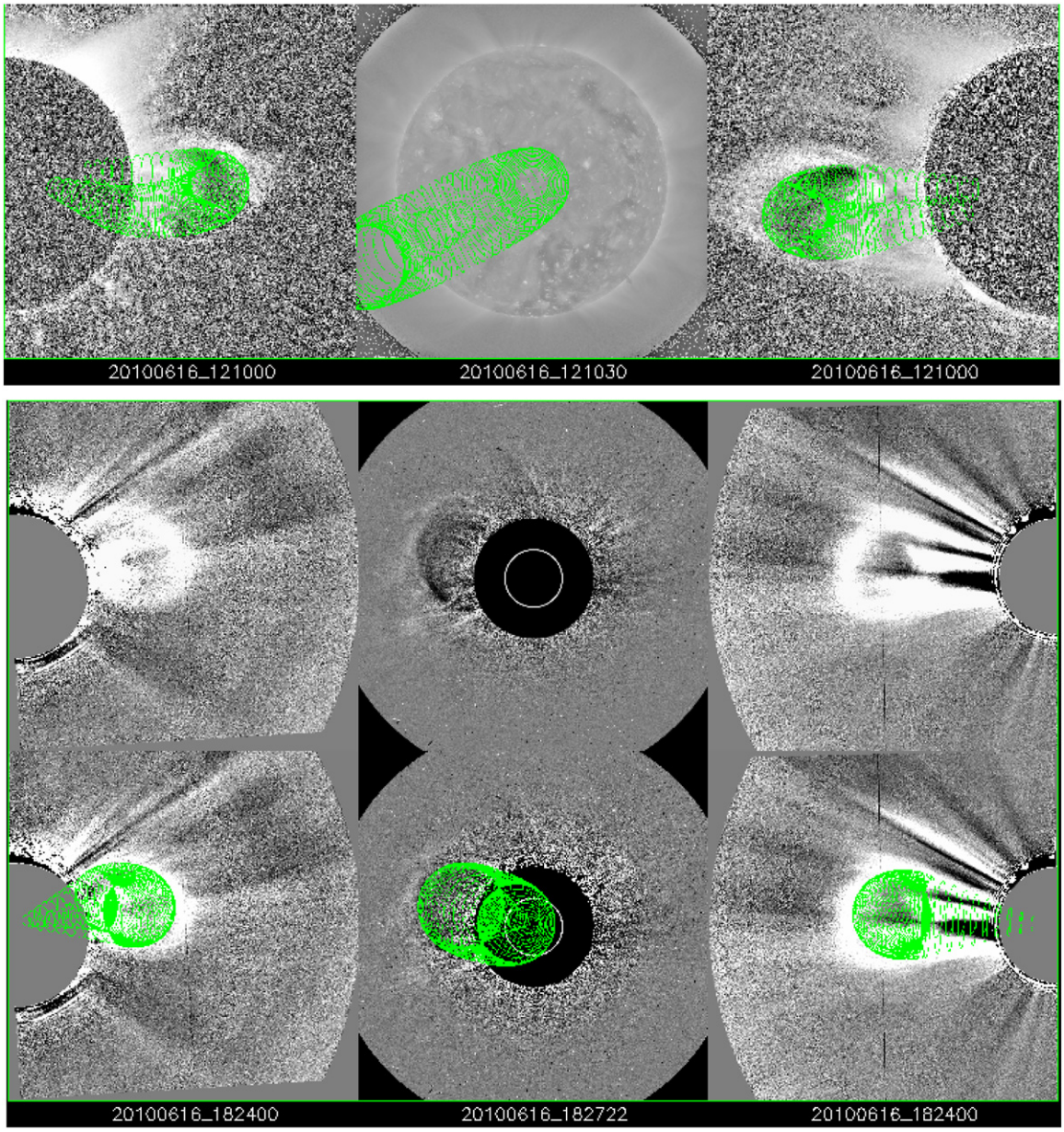

Figure 2. Representative GCS model fits to the SECCHI and LASCO images using the Thernisien et al. (2009) forward-fitting procedure at two times during the evolution of the CME in the low corona. Top panel: COR1-B (left), AIA-193 (middle), COR1-A (right). Middle panel: COR2-B (left), LASCO-C2 (middle), COR2-A (right). Bottom panel: the same images with the GCS model superimposed. The times are shown at the bottom of each frame. The frames were extracted from the online movie.

(An animation of this figure is available in the online journal.)

The filament originated from a long, quiet-Sun, neutral line in the southern hemisphere close to the central meridian. The filament itself was not visible in the AIA images, most likely because it was thin and was situated high in the corona. After some search, we were able to locate in the AIA 171 Å images the weak filament flows seen in the EUVI 304 Å channel. We used the apparent locus of these flows as the northern footpoint of the erupted flux rope (Figure 1, top left, upper red circle). We also found a very faint and diffuse loop arcade, best seen in AIA 211 Å around 1211 UT, which marked the southern footpoint (Figure 1, top left, lower red circle). Based on these observations, we estimated the length of the erupted neutral line (0.25 $R_\odot$) and its orientation (38° counterclockwise (CCW) from the solar equator). The erupted flux rope was right handed based on the HMI photospheric magnetogram and the location of the footpoints of the erupted flux rope. No events (e.g., flares, filament disappearances, etc.) were reported in any wavelength on this day from any solar monitoring service.

2.1. 3D Reconstruction of the Rotating CME

The CME exhibits a very clear flux-rope structure in the COR2 images, especially in COR2-A. However, even a quick-look movie of the event shows a very peculiar behavior. The CME seems to overexpand and flatten as it propagates within the COR2 field of view. As we discussed earlier, overexpanding CMEs at heights above 5 $R_\odot$ are a rare phenomenon. This is clearly an Earth-directed CME. It appeared in LASCO/C2 as a partial halo at 14:54 UT.

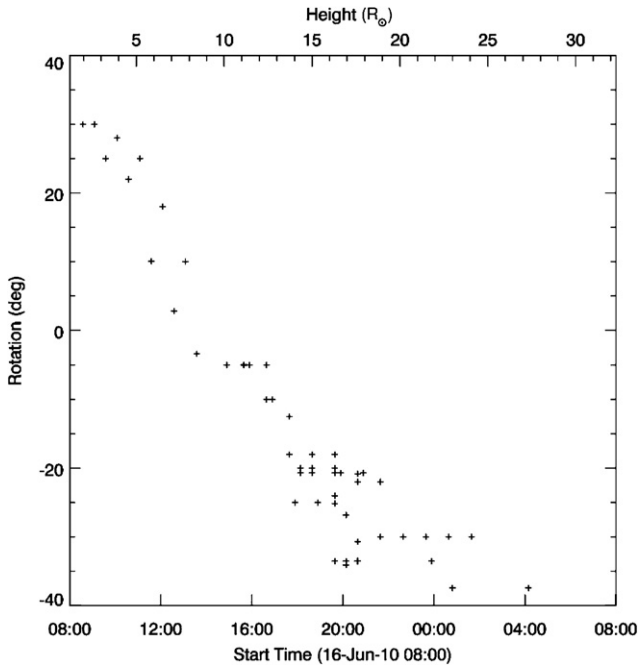

Figure 3. CME rotation as a function of time and heliocentric radial distance (top axis). The rotation is derived from the GCS fits to SECCHI/COR2-A, B, and LASCO/C2, C3 for heights above 3 $R_\odot$ and GCS fits to SECCHI/COR1-A and B for heights below 3 $R_\odot$. Positive angles correspond to counterclockwise rotation relative to the solar equator.

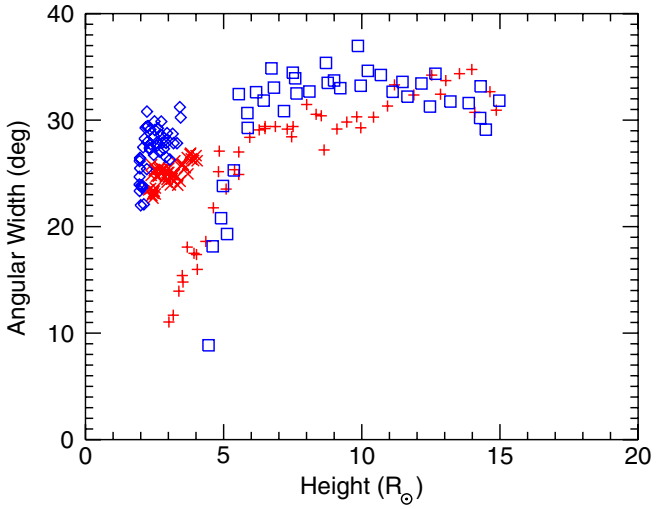

Figure 4. Projected CME angular width as a function of projected height as measured from COR1-A (red stars) and COR2-A (red crosses), and COR1-B (blue diamond) and COR2-B (blue squares). The occultation of the main CME body by the COR2 occulter is responsible for the discrepancy between the COR1 and COR2 measurements below 5 $R_\odot$. The angular width increases by only 10° between 2 and 15 $R_\odot$. Thus, it is difficult to ascertain the rotation of the CME from single viewpoint measurements alone.

We derived the 3D properties of the CME using the Thernisien et al. (2009) technique, which is the standard analysis procedure for 3D reconstruction of SECCHI data. In brief, the technique consists of using the Graduated Cylindrical Shell (GCS) model, which is a geometric representation of an idealized flux rope, to simultaneously fit two or three nearly coincident views of an event. In our case, we used COR1, COR2, HI-1, C2, and C3 observations of the CME to fit and track the evolution of the CME shape as it propagated outward. In this Letter, we discuss the CME evolution only up to the edge of the COR2 field of view (15 $R_\odot$). All fits were made "by eye" and to allow the reader to judge the success of the fit, we have assembled representative snapshots into an accompanying online animation. A single frame from that animation is shown in Figure 2. The top panels show the COR2-B, C2, and COR2-A images and the lower panels show the same images but with the GCS model superimposed. Note that we are trying to fit the flux rope (cavity) and not the leading edge of the CME, which is due to material pileup in front of the flux rope. At lower heights, where LASCO images are unavailable, we use the COR1-A and B images and project the fit onto an AIA 193 Å image. This allows the viewer to easily compare the orientation of the ejected structure to that of the source region. The movie demonstrates that we had to impose a strong rotation to the GCS model in order to simultaneously fit all three viewpoints. We note that the LASCO views are essential in determining the orientation of the structure because of its symmetry relative to the COR2 views. We would not be able to get such robust determination of the rotation without the LASCO observations. Vice versa, the single viewpoint LASCO observations cannot establish reliably a rotation to the halo CME.

3. RESULTS

The fitting with the GCS model returns several parameters regarding the CME dimensions and its location in 3D space. The CME rotation is our prime focus here and we plot it as a function of the radial heliocentric distance in Figure 3. Positive angle corresponds to CCW rotation relative to the solar equator. Hence, the CME is rotating clockwise according to Figure 3 and the online animation. This is exactly the expected sense of rotation for right-handed flux ropes (Lynch et al. 2009). Our first measurement shows a 30° tilt at 2–3 $R_\odot$. This angle is very similar to the orientation of the neutral line on the surface (37°), implying negligible rotation below 3 $R_\odot$. This result seems to contradict the amount of rotation deduced from filament observations. For example, Lynch et al. (2009) predicted rotations of 40°–50° below 2 $R_\odot$. However, our event started at a larger height and was not associated with an active region filament. We would expect that events from stronger magnetic field region would exhibit stronger rotations at lower heights. Our CME rotated very strongly, by about 35° within the first 5 $R_\odot$ and then began to slow down. The overall amount of rotation is very high, at about 60° day^{-1}. In contrast, Lynch et al. (2010) reported only 24° day^{-1} for the 2008 June 2 event.

We also examine the angular expansion of the CME as seen from the individual *STEREO* viewpoints. In this way, we can relate the rotation results from the 3D fitting to past experience based on single viewpoint observations. Figure 4 shows the height variation of the projected angular width in COR1-A and COR2-A (red stars and crosses, respectively) and in COR1-B and COR2-B (blue diamond and squares, respectively). The discrepancy, below 5 $R_\odot$, between the COR1 and COR2 measurements is due to the occultation of the main CME body by the COR2 occulter at these heights. For both viewpoints, the total change in the angular width is only 10° from 2 to 15 $R_\odot$. This is a very modest change, especially when we consider the large rotation derived from the multi-viewpoint observations. It goes a long way toward explaining the lack of CME rotation reports in the past. Angular width changes of the order of 10° can easily be overlooked or attributed to measurement errors, without compelling indications for rotation. The latter are

unlikely to come about from single viewpoint observations. Even in our case, the two-viewpoint SECCHI observations were insufficient (due to their viewing symmetry relative to the event) for establishing conclusively the CME rotation. The addition of the LASCO viewpoint was essential for clarifying the CME tilt and for verifying the rotation measurements.

The large angular rotation speed makes this event quite unusual. It is also intriguing that this CME shares many common characteristics with the 2008 June 2 CME which is also the only other event with strong rotation. Why does a quiet-Sun CME from a very low field region exhibit such strong rotation? Why does it rotate so vigorously in the outer corona instead of the lower corona where magnetic fields are stronger? Why does it continue to rotate beyond 15 $R_\odot$? The tendency of rotating CMEs to originate in low magnetic field regions makes difficult an explanation due to Lorentz forces within or around the flux rope as have been suggested (e.g., Isenberg & Forbes 2007; Lynch et al. 2009). However, one cannot exclude the role of reconnection with the ambient field which could also lead to strong rotation (Shiota et al. 2010) even in the presence of weak fields, as long as the gas pressure is small the magnetic pressure. These questions can only be answered by detailed theoretical and numerical modeling which is beyond the scope of this Letter. We can only offer some suggestions based on the observations reported here.

The time series of the observations from the three EUV telescopes show that the southern end of the CME left earlier than the northern part and that the eruption proceeds from southwest to northeast in an unzipping fashion. The highly detailed structure in the COR2 images suggests a very well formed flux rope above the filament and hence the presence of significant self-helicity. Taken together, the observations indicate an untwisting flux rope with one of its footpoints possibly disconnected from the low corona. That may allow the overall structure to unwrithe much more easily than shown in the simulations where both footpoints are line-tied to the photosphere (Lynch et al. 2009). Such a simulation would be instructive. The similarities between the 2008 June 2 and this event extend also to the 2008 November 2 polar crown filament eruption we examined in Kilpua et al. (2009). The latter exhibited strong unwrithing, and 304 Å downward flows very similar to our event, but was oriented normal to the other two eruptions. However, the November 2 CME did show a strong flattening of the front in the COR2 and HI1 images. At the time, we considered the interaction with a previous CME as the source of that flattening but we may need to revisit that interpretation. In any case, there seems to be a hint of correlation between the eruptions from large, quite-Sun neutral lines and strong rotation in the outer corona.

4. CONCLUSIONS

In summary, we have reported the first unambiguous observation and measurement of a rotating CME in the outer corona. We find a rotation speed of 60° day^{-1} starting at 2 $R_\odot$. The rotation slows down but continues beyond the COR2 field of view. We require the use of simultaneous observations from three viewpoints (SECCHI-A, B, and LASCO) to conclusively establish and measure the CME rotation. We suggest that these strong rotations might be a characteristic of eruptions from neutral lines in the quiet Sun. We propose that the rotation is not driven by Lorentz forces but may be related to the disconnection of one of the flux-rope footpoints early in the eruption which allows the whole structure to unwrithe.

We are also able to determine that the nonlinear expansion of CMEs, as derived by a variable projected angular width, can be a projection effect related to the rotation of the structure in the coronagraph (and in the heliospheric imager, not shown here) fields of view. However, the degree of nonlinear expansion does not correlate strongly with the amount of rotation. We find that, in our event, the projected angular width varies by only 10° between 2 and 15 $R_\odot$ while it rotates by 60° over the same height range. If this result holds for other events, it will clarify the prevalency of constant angular width measurements and the lack of detection of CME rotation in the past. Simply put, the effect of rotation on the CME projection is too weak to be determined conclusively from single viewpoint observations.

Our results have also clear implications for space weather. First of all, they demonstrate the power of coronagraph measurements from multiple vantage points and especially from points away from the Sun–Earth line. This event was a faint halo in the LASCO images and disappeared relatively quickly from the C3 field of view. Second, if rotations are indeed common during the CME propagation and if they continue to large distances, then prediction of the direction of the magnetic field entrained in the CME flux rope will be more difficult than anticipated. Theoretical investigations need to focus on this aspect to be able to make progress on space weather prediction. Lastly, the question remains whether this is a common occurrence for CMEs in general or for CMEs from the quiet Sun in particular.

We were fortunate that this CME was intercepted by both the *MESSENGER* and *Wind* in situ instruments so its evolution to 1 AU can be studied. We will report these results in a forthcoming paper (Nieves-Chinchilla et al. 2011).

We thank O. C. St. Cyr for useful discussions. The AIA data used here are courtesy of *SDO* (NASA) and the AIA consortium. The SECCHI data are courtesy of *STEREO* (NASA) and the SECCHI consortium. A.V.'s work is supported by NASA grant NNH08AI50I.

REFERENCES

Byrne, J. P., Gallagher, P. T., McAteer, R. T. J., & Young, C. A. 2009, A&A, 495, 325
Funsten, H. O., Gosling, J. T., Riley, P., Cyr, O. C. S., Forsyth, R. J., Howard, R. A., & Schwenn, R. 1999, J. Geophys. Res., 104, 6679
Howard, R. A., et al. 2008, Space Sci. Rev., 136, 67
Isenberg, P. A., & Forbes, T. G. 2007, ApJ, 670, 1453
Kaiser, M. L., Kucera, T. A., Davila, J. M., St. Cyr, O. C., Guhathakurta, M., & Christian, E. 2008, Space Sci. Rev., 136, 5
Kilpua, E. K. J., et al. 2009, Ann. Geophys., 27, 4491
Lynch, B. J., Antiochos, S. K., Li, Y., Luhmann, J. G., & DeVore, C. R. 2009, ApJ, 697, 1918
Lynch, B. J., Li, Y., Thernisien, A. F. R., Robbrecht, E., Fisher, G. H., Luhmann, J. G., & Vourlidas, A. 2010, J. Geophys. Res. (Space Phys.), 115, 7106
Nieves-Chinchilla, T., Colaninno, R., Vourlidas, A., & Szabo, A. 2011, ApJ, in press
Poomvises, W., Zhang, J., & Olmedo, O. 2010, ApJ, 717, L159
Robbrecht, E., Patsourakos, S., & Vourlidas, A. 2009, ApJ, 701, 283
Shiota, D., Kusano, K., Miyoshi, T., & Shibata, K. 2010, ApJ, 718, 1305
St. Cyr, O. C., et al. 2000, J. Geophys. Res., 105, 8169
Stenborg, G., Vourlidas, A., & Howard, R. A. 2008, ApJ, 674, 1201
Stockton-Chalk, A. 2002, in Solspa 2001, Proc. Second Solar Cycle and Space Weather Euroconference, ed. H. Sawaya-Lacoste (ESA SP-477; Noordwijk: ESA), 277
Thernisien, A., Vourlidas, A., & Howard, R. A. 2009, Sol. Phys., 256, 111
Torok, T., Kliem, B., Thompson, W. T., & Berger, M. A. 2010, AGU Fall Meeting Abstracts, #SH43C-01

Vourlidas, A., & Ontiveros, V. 2009, in AIP Conf. Ser. 1183, Shock Waves in Space and Astrophysical Environments, ed. X. Ao & G. Z. R. Burrows (Melville, NY: AIP), 139
Webb, D. F., & Jackson, B. V. 1990, J. Geophys. Res., 95, 20641
Webb, D. F., Kahler, S. W., McIntosh, P. S., & Klimchuck, J. A. 1997, J. Geophys. Res., 102, 24161
Xie, H., Ofman, L., & Lawrence, G. 2004, J. Geophys. Res. (Space Phys.), 109, 3109
Xue, X. H., Wang, C. B., & Dou, X. K. 2005, J. Geophys. Res. (Space Phys.), 110, 8103
Yurchyshyn, V. 2008, ApJ, 675, L49
Yurchyshyn, V., Hu, Q., Lepping, R. P., Lynch, B. J., & Krall, J. 2007, Adv. Space Res., 40, 1821
Zhao, X. P., Plunkett, S. P., & Liu, W. 2002, J. Geophys. Res. (Space Phys.), 107, 1223